Fuel 93 (2012) 692–702

Contents lists available at SciVerse ScienceDirect

Fuel

journal homepage: www.elsevier.com/locate/fuel

Sequential pyrolysis of willow SRC at low and high heating rates – Implications for selective pyrolysis

C.E. Greenhalf, D.J. Nowakowski *, A.B. Harms, J.O. Titiloye, A.V. Bridgwater

Aston University Bioenergy Research Group, School of Engineering and Applied Science, Aston University, Birmingham B4 7ET, United Kingdom

ARTICLE INFO

Article history:
Received 16 February 2011
Received in revised form 17 November 2011
Accepted 21 November 2011
Available online 4 December 2011

Keywords:
TGA
Py–GC–MS
Fast pyrolysis
Slow pyrolysis
Bio-oil

ABSTRACT

The main aim of the work is to investigate sequential pyrolysis of willow SRC using two different heating rates (25 and 1500 °C/min) between 320 and 520 °C. Thermogravimetric analysis (TGA) and pyrolysis – gas chromatography – mass spectroscopy (Py–GC–MS) have been used for this analysis. In addition, laboratory scale processing has been undertaken to compare product distribution from fast and slow pyrolysis at 500 °C. Fast pyrolysis was carried out using a 1 kg/h continuous bubbling fluidized bed reactor, and slow pyrolysis using a 100 g batch reactor. Findings from this study show that heating rate and pyrolysis temperatures have a significant influence on the chemical content of decomposition products. From the analytical sequential pyrolysis, an inverse relationship was seen between the total yield of furfural (at high heating rates) and 2-furanmethanol (at low heating rates). The total yield of 1,2-dihydroxybenzene (catechol) was found to be significant higher at low heating rates. The intermediates of catechol, 2-methoxy-4-(2-propenyl)phenol (eugenol); 2-methoxyphenol (guaiacol); 4-Hydroxy-3,5-dimethoxybenzaldehyde (syringaldehyde) and 4-hydroxy-3-methoxybenzaldehyde (vanillin), were found to be highest at high heating rates. It was also found that laboratory scale processing alters the pyrolysis bio-oil chemical composition, and the proportions of pyrolysis product yields. The GC–MS/FID analysis of fast and slow pyrolysis bio-oils reveals significant differences.

1. Introduction

The finite character of fossil fuels and their contribution to anthropogenic carbon dioxide emissions, has led to intense research activities in the field of renewable resources and energy. This has received considerable attention worldwide since the oil crisis in the 1970s. Environmental concerns globally are the driving force behind recent efforts to develop alternative energy sources that are renewable. Biomass is a promising source of renewable energy; this paper therefore focuses on the potential of willow short rotation coppice (SRC) as a renewable source of fuel and chemicals. Willow SRC is mainly grown in the northern hemisphere, and is potentially suitable as a renewable energy crop, because it grows relatively fast, requires low agro-chemical inputs, and has an energy balance of 20:1 (20 times more energy is obtained than used to grow it) [1].

Fast pyrolysis processing maximises the yield of liquid products from biomass (up to 75 wt.%), and produces some gas and solid by-products. The principles of fast pyrolysis and the utilisation of its products are the content of many publications. A comprehensive review has been conducted by Bridgwater [2]. For the fast pyrolysis process, it is essential to achieve both high heat transfer and heating rates (>1000 °C/s), well-controlled temperature, short hot vapour residence times (<2 s) and rapid cooling of the vapours [3]. Fluidized bubbling bed reactors have these key elements, and are a well-established technology [4]. Furthermore, they do not have any rotating internal parts that are subject to wear or are difficult to seal.

Alén et al. [5] reported from a number of studies that the thermal decomposition products of hemicellulose, cellulose and lignin can be divided into major groups. The major groups for cellulose include: (1) Light volatiles (i.e. carbon monoxide, carbon dioxide, methanol, acetaldehyde and hydroxacetaldehyde); (2) Anhydroglucopyranose (1,6-anhydro-β-D-glucopyranose); (3) Anhydroglucofuranose (1,6-anhydro-β-D-glucofuranose); (4) Dianhydroglucopyranose (1,4:3,6-dianhydro-α-D-gludopyranose; (5) Furans (i.e. (2H)-furan-3-one and 5-hydroxymethyl-3-furaldehyde); and (6) Other products (mainly pyrans). From this study, they concluded that the main products formed between 400 and 600 °C were anhydrosugars (groups 2, 3 and 4), mainly levoglucosan. At higher temperatures (600–1000 °C), light volatiles were predominantly formed (group 1). Thermal decomposition of cellulose is extremely complex, but initial break-down starts with the polymer chain prior to the cracking of glycosidic bonds between neighbouring pyrans, due to weak bonds [6]. This can be seen in Fig. 1.

* Corresponding author.
E-mail address: d.j.nowakowski@aston.ac.uk (D.J. Nowakowski).

0016-2361/$ - see front matter © 2011 Elsevier Ltd. All rights reserved.
doi:10.1016/j.fuel.2011.11.050

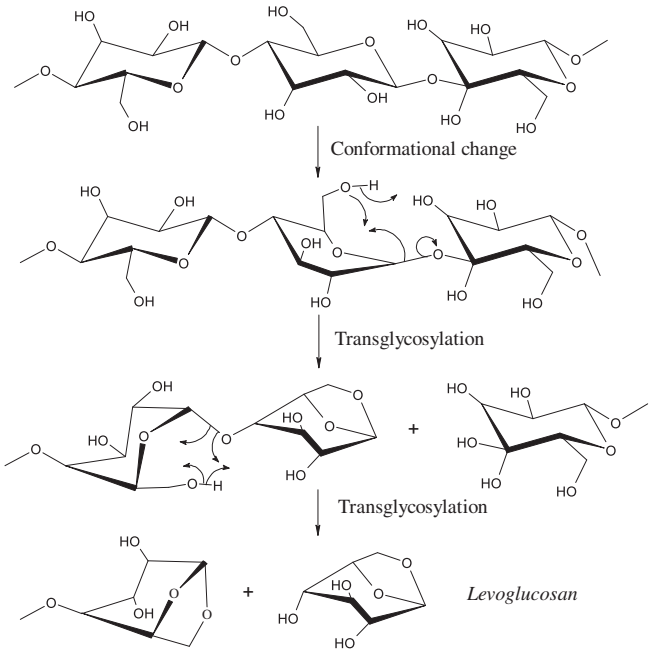

Fig. 1. Pyrolytic formation of levoglucosan from cellulose.

A number of models have been proposed to account for the decomposition mechanism of pure cellulose at high and low temperatures. A good example is the Waterloo model [7], and the Piskorz et al. model [8], which is a more recent modification of the Bradbury et al. model [9]. Another well-known model is the Broido-Shafizadeh model [9] recently adapted and updated by Liao et al. [10] to include further modifications. It should be emphasised that these models primarily concentrate on the more immediate decomposition products of pure cellulose, but that secondary decomposition pathways play an important role on the final product distribution. For example, an increase in hot vapour residence time during pyrolysis, will result in an elevated low molecular weight gas yield [10], as a result of increased secondary decomposition reactions. Further details for these models can be found in the literature [7–14]. The general consensus among these investigators with respect to the thermal decomposition of cellulose can be found in Fig. 2, and this shows two competing pyrolytic decomposition routes. The first route involves the dehydration of cellulose to yield an '*anhydrocellulose*' (or 'active cellulose'), and the second results in the depolymerisation of cellulose to yield primarily levoglucosan, with minor amounts of other anhydromonosaccacharides. The k_A route in Fig. 2 is promoted at low temperatures and low heating rates, while the k_B route becomes the major decomposition pathway at higher temperatures and high heating rates.

Thermal decomposition of hemicellulose is usually analogous to cellulose, and the major groups are categorised by Alén et al. [5]: (1) Light volatiles, (2) Anhydroglucopyranose, (3) Other anhydroglucoses, (4) Other anhydrohexoses, (5) Levoglucosenone, (6) Furans and (7) Other products. The thermal stability is much lower than that of cellulose. This is due to the lack of crystallinity and short side chains, which crack easily, resulting in depolymerisation and intramolecular dehydration reactions [5,6].

Alén et al. [5] found that thermal decomposition of lignin could be divided into 8 major groups, namely; (1) Light volatiles; (2) Catechols; (3) Vanillins; (4) Others guaiacol; (5) Propyl guaiacols; (6) Others phenols; (7) Aromatic hydrocarbons; and (8) Others. Groups 3, 4 and 5 are largely predominant from 400 to 800 °C, while group 1 became dominant after 800 °C. The decomposition occurs over a wide temperature range, and breakdown is thought to be the result of side chain cracking and condensation reactions [6]. Fig. 3 shows a fragment of the lignin polymer structure with β-O-4 ether bond [15].

Research into pyrolysis product distribution is very important because it is an essential step required to improve product quality and optimise processing facilities. The mechanisms of pyrolytic decomposition of biomass are still not well understood, due to both the overwhelmingly complex biomass chemistry and the capability limits of analytical instrumentation [7,16]. In addition, pyrolysis products are known to have low thermal stability, and this can cause further analysis issues, due to premature chemical changes in the usual high temperature environment of many analytical procedures. The mechanisms involved in chemical changes and chemical production during pyrolysis are also extremely difficult to determine. For this reason, the focus of the present study is to examine how changes in pyrolysis product composition can be achieved by modification of pyrolysis temperature and heating rates using analytical equipment. Thermogravimetric analysis is reliable analytical technique used by a number of researchers to investigate the thermal characteristics of various materials [11,17–24]. This technique however, does not give any indication of the individual compounds produced during different temperature regions on the thermogravimetric curve. Pyrolysis – gas chromatography – mass spectroscopy (Py–GC–MS) can be used in conjunction to TGA to gain a deeper insight into the decomposition products.

The purpose of this research is to investigate how light and medium volatile decomposition products alter with temperature and heating rate (sequential pyrolysis). This has been undertaken using a single biomass sample for each heating rate of 25 and 1500 °C/min, over eight different pyrolysis temperatures (in a step sequence) ranging from 320 to 520 °C by analytical Py–GC–MS. In addition, laboratory scale processing has been undertaken to compare fast and slow pyrolysis product yields and bio-oil chemical composition by GC with mass (MS) and flame ionisation (FID) detection.

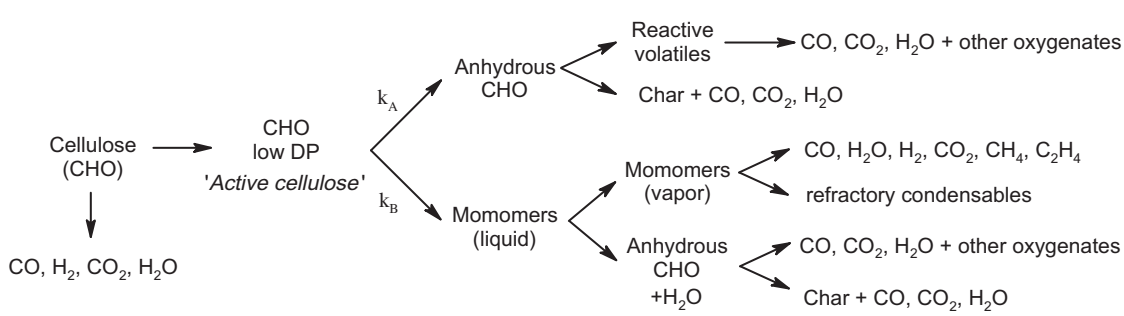

Fig. 2. Scheme of cellulose pyrolysis.

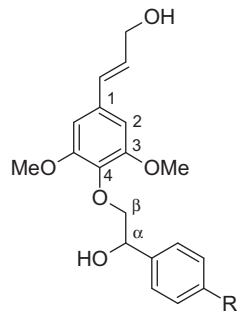

Fig. 3. Fragment of lignin polymer structure with β-O-4 ether bond.

2. Experimental

2.1. Materials

The willow SRC sample was obtained from Rothamsted Research in Harpenden, Hertfordshire, England. The willow sample was dried and ground and the following particle size fractions were prepared for analysis; TGA and Py–GC–MS analyses – 150–250 μm, fast pyrolysis and slow pyrolysis reactors – 0.25–1.00 mm. For TGA and Py–GC–MS analyses a biomass splitter was used to obtain a representative sample.

2.2. Methodology

2.2.1. Thermogravimetric analysis (TGA)

Thermogravimetric analysis was undertaken using a PerkinElmer Pyris 1 analyser, following the E1131-03 ASTM standard [25]. A sample of approximately 3 mg was pyrolysed to the maximum temperature of 900 °C at a heating rate of 25 °C/min, with a nitrogen purge at a flow rate of 30 ml/min and hold time of 15 min. The ash content was investigated in an air atmosphere at the maximum temperature of 575 °C, with a hold time of 15 min at a heating rate of 5 °C/min at a purge rate of 30 ml/min.

Table 1
Proximate analysis, ultimate analysis, inorganic analysis and higher heating value of willow SRC.

Ultimate analysis%[(d.b)]		Inorganic analysis[(d.b)]	ppm
C	48.48	Al	277
H	5.74	As	–
N	1.87	Ca	11,546
O[a]	43.91	Cd	–
		Co	–
Proximate analysis%		Cr	–
Moisture	5.71	Cu	11
Volatile matter[(d.b)]	78.59	Fe	240
Fixed carbon[(d.b)]	16.04	K	5883
Ash[(d.b)]	5.38	Mg	1590
		Mn	118
Higher heating value[(d.b)]		Mo	–
(MJ/kg)	19.12	Na	118
		Ni	–
		P	1884
		Pb	–
		S	1423
		Se	–
		Ti	5
		Zn	202

– Not detected.
d.b – dry bases.
[a] Oxygen by difference.

2.2.2. Elemental analysis and higher heating value

The elemental analysis for carbon, hydrogen and nitrogen was carried out by external laboratory using a Carlo-Erba 1108 elemental analyser EA1108. Carbon, hydrogen and nitrogen were analysed

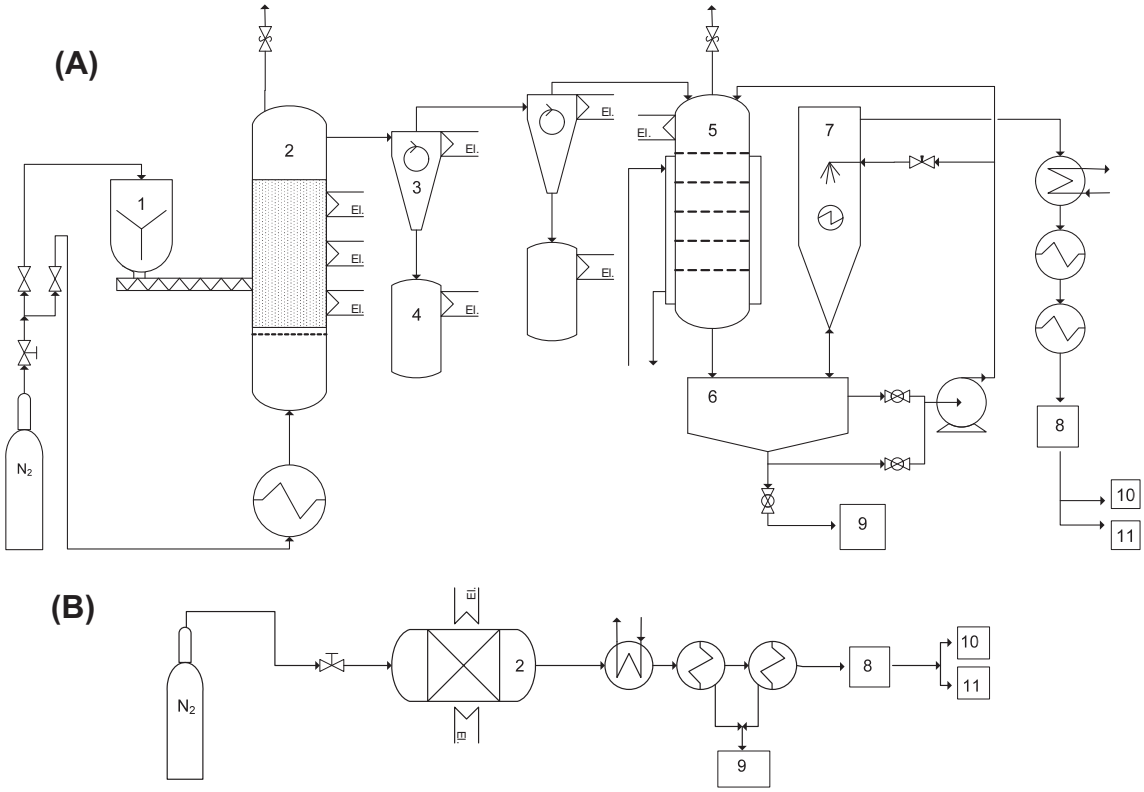

Fig. 4. Flow diagrams of the fast (A) and slow (B) pyrolysis rigs. 1 – feed hopper, 2 – reactor, 3 – cyclone, 4 – char pot, 5 – quench column, 6 – common tank,7 – electrostatic precipitator, 8 – gas counter, 9 – liquid out, 10 – GC, 11 – gas out.

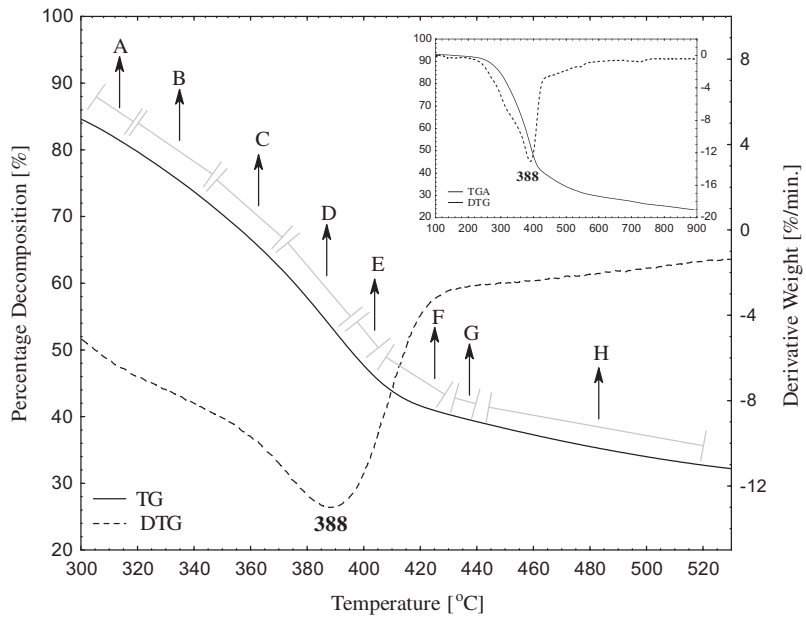

Fig. 5. Chemical decomposition products investigated (A–H) of willow SRC. A–H are indicative of pyrolysis region temperatures.

in duplicate and average values were taken. A PerkinElmer Optima 7300DV Induced Coupled Plasma (ICP) Emission Spectrometer was used to determine the inorganic content by digesting the biomass sample in a mixture of nitric and perchloric acids (for 14 hours at 80 °C), and the solution was analysed in triplicate. The higher heating value (HHV) was obtained using the following equation [26]:

$$\text{HHV (MJ/kg)} = 0.3491 \cdot \text{C} + 1.1783 \cdot \text{H} + 0.1005 \cdot \text{S} - 0.1034 \cdot \text{O} - 0.0151 \cdot \text{N} - 0.0211 \cdot \text{Ash} \quad (1)$$

O% oxygen by difference, C, H, N and O wt.% on dry basis.

2.2.3. Pyrolysis – gas chromatography – mass spectrometry (Py–GC–MS)

2.2.3.1. Analytical pyrolysis. Analytical stage pyrolysis between 320 and 520 °C was investigated using two different heating rates: 25 °C/min (to represent slow pyrolysis) and 1500 °C/min (to represent fast pyrolysis). A single sample of approximately 3 mg was used for the eight stages of the pyrolysis experiment with the following pyrolysis temperature steps: 320, 350, 370, 390, 405, 420, 435 and 520 °C. Py–GC–MS tests were performed on each sample using a CDS 5200 pyrolyser coupled to a Varian GC-450 chromato-

Table 2
Yields of quantified compounds at two heating rates (25 and 1500 °C/min).

	(wt.%^{daf}, heating rate – 25 °C/min)								
	320 °C	350 °C	370 °C	390 °C	405 °C	420 °C	435 °C	520 °C	Total 320–520 °C
Furfural	0.044	0.143	0.082	0.105	0.033	–	–	–	0.407
2-Furanmethanol	0.042	0.103	0.134	0.240	0.048	0.030	–	–	0.596
Phenol	0.015	0.044	0.036	0.035	0.056	0.017	0.011	0.012	0.227
Guaiacol	0.013	0.019	0.027	0.042	0.051	0.014	0.012	–	0.179
2-Methoxy-4-methylphenol	–	–	0.012	0.027	0.034	0.007	–	–	0.081
Catechol	0.111	0.238	0.198	0.215	0.187	0.089	0.080	0.068	1.186
3-Methoxycatechol	0.019	0.020	0.029	0.055	0.065	0.018	0.017	0.017	0.240
1,2,4-Trimethoxybenzene	–	–	0.023	0.029	0.024	–	–	–	0.076
2-Methoxy-4-vinylphenol	0.019	0.059	0.087	0.082	0.035	–	–	–	0.282
Eugenol	–	0.038	0.027	0.016	–	–	–	–	0.081
Vanillin	0.013	0.018	0.017	–	–	–	–	–	0.048
Levoglucosan	–	0.062	0.088	0.274	0.112	–	–	–	0.536
Syringaldehyde	–	0.025	0.021	0.015	–	–	–	–	0.061
Total									**4.000**
	(wt.%^{daf}, heating rate – 1500 °C/min)								
Furfural	0.039	0.191	0.126	0.162	–	–	–	–	0.518
2-Furanmethanol	0.037	0.077	0.102	0.181	0.150	–	–	–	0.547
Phenol	0.016	0.041	0.043	0.037	0.058	0.018	0.014	0.016	0.242
Guaiacol	0.015	0.026	0.032	0.045	0.076	0.020	0.015	–	0.229
2-Methoxy-4-methylphenol	–	0.010	0.015	0.027	0.053	0.011	0.009	0.010	0.134
Catechol	–	0.041	0.052	0.080	0.105	–	–	–	0.278
3-Methoxycatechol	–	–	0.024	0.040	0.086	0.020	–	–	0.170
1,2,4-Trimethoxybenzene	–	–	0.018	0.029	0.040	0.012	0.011	–	0.110
2-Methoxy-4-vinylphenol	0.016	0.045	0.071	0.094	0.076	0.014	0.012	–	0.329
Eugenol	0.011	0.031	0.032	0.026	0.016	0.009	–	–	0.126
Vanillin	0.012	0.017	0.019	0.022	–	–	–	–	0.070
Levoglucosan	–	0.047	0.071	0.123	0.385	–	–	–	0.626
Syringaldehyde	–	0.027	0.026	0.020	0.016	–	–	–	0.090
Total									**3.470**

– Not detected; daf – dry ash free.

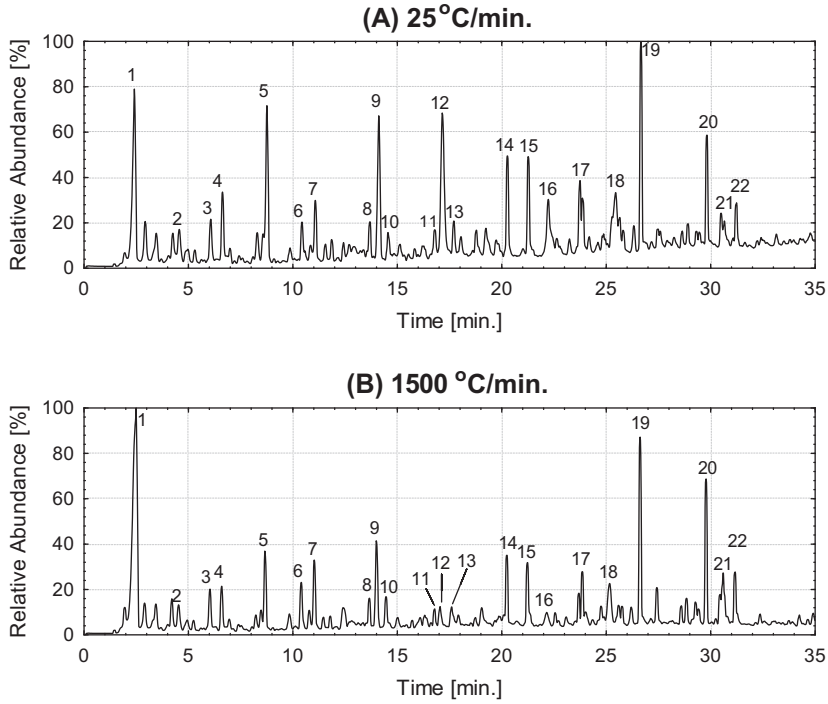

Fig. 6. Chromatograms for stage pyrolysis of willow SRC at 370 °C using two heating rates: 25 °C/min (A) and 1500 °C/min (B). *Peak assignments*: (1) Acetic acid; (2) Toluene; (3) Furfural; (4) 2-Furanmethanol (5) 1,2-Cyclopentanedione; (6) Phenol; (7) 3,4-Dihydroxy-3′-cyclobutene-1,2-diol; (8) 2-Methoxyphenol; (9) Cyclopropylcarbinol; (10) 5-(Hydroxyl)-2-furancarboxaldehyde; (11) 2-Methoxy-4-methyl-phenol; (12) 1,2-Benzenediol; (13) 1,2,4-Trimethoxybenzene; (14) 2-Methoxy-4-vinylphenol; (15) 2,6-Dimethoxy-phenol; (16) 4-Ethylcatechol or/and 4-Ethyl-1,3-benzenediol; (17) 1,4:3,6- Dianhydro-α-D-glucopyranose; (18) 1,6-Anhydro-β-D-glucopyranose (levoglucosan); (19) 3′5′-Dimethoxyacetophenone; (20) 2,6-Dimethoxy-4-(2-propenyl)-phenol; (21) 4-Hydroxyl-2-methoxycinnamaldehyde; (22) Desaspidinol.

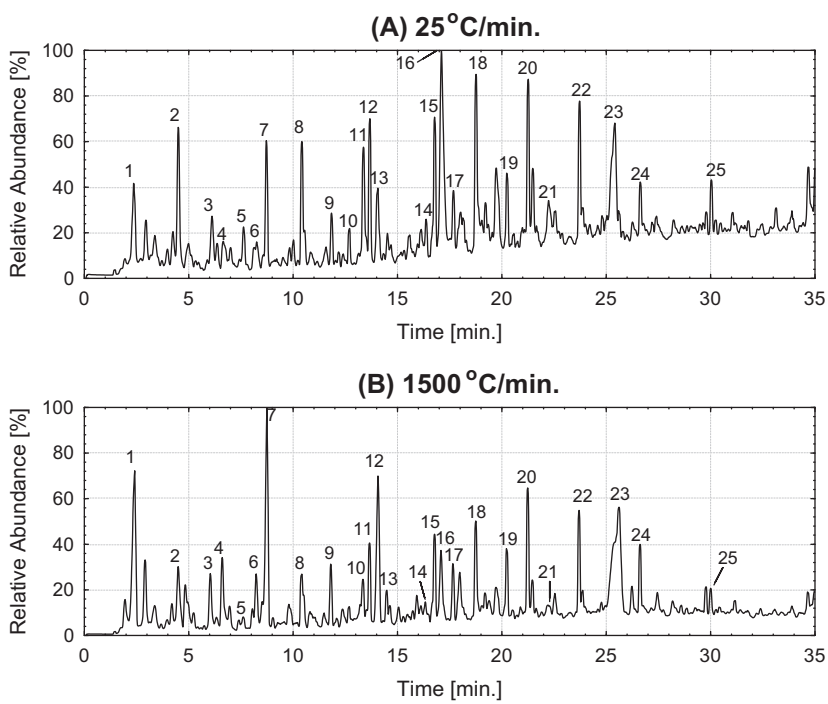

Fig. 7. Chromatograms for stage pyrolysis of willow SRC at 405 °C using two heating rates: 25 °C/min (A) and 1500 °C/min (B). *Peak assignments*: (1) Acetic acid; (2) Toluene; (3) Furfural; (4) 2-Furanmethanol; (5) Cyclohexanone; (6) 2(5H)-Furanone; (7) 1,2-Cyclopentanedione and/or 1,3-Cyclopentanedione; (8) Phenol; (9) 3-Methyl-1,2-cyclopentanedione; (10) 2-Methylphenol; (11) 2-Methoxyphenol; (12) Cyclopropylcarbinol; (13) 5-(Hydroxyl)-2-furancarboxaldehyde; 14) 3-Ethylphenol or/and4-Ethylphenol; 15) 2-Methoxy-4-methyl-phenol; (16) 1,2-Benzenediol and/or Resorcinol; (17) 1,2,4-Trimethoxybenzene; (18) 3-Methoxy-1,2-dibenzenediol; (19) 2-Methoxy-4-vinylphenol; (20) 2,6-Dimethoxy-phenol; (21) 4-Ethylcatechol or/and 4-Ethyl-1,3-benzenediol; (22) 1,4:3,6- Dianhydro-α-D-glucopyranose; (23) 1,6-Anhydro-β-D-glucopyranose (levoglucosan); (24) 3′,5′-Dimethoxyacetophenone; (25) 2,6-Dimethoxy-4-(2-propenyl)-phenol.

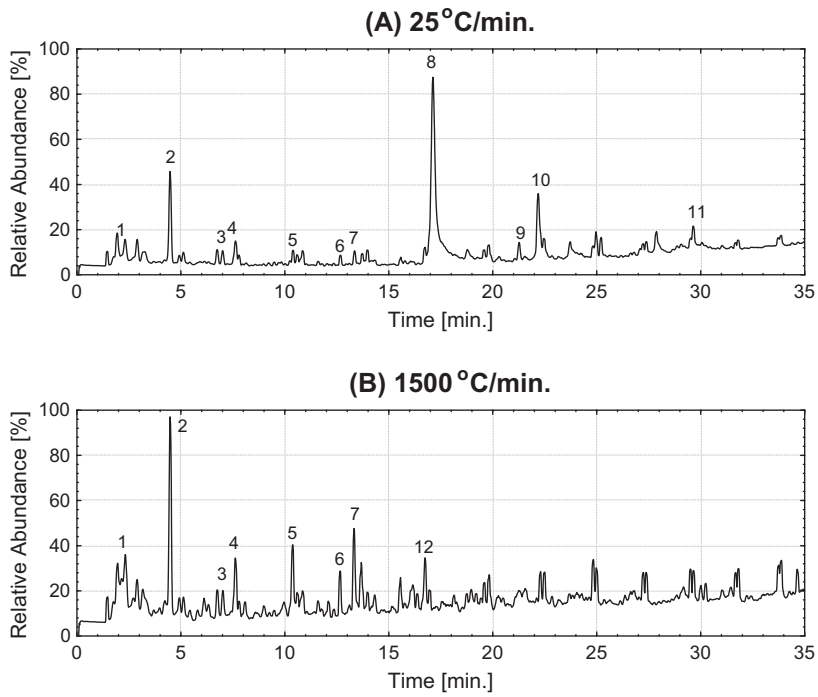

Fig. 8. Chromatograms for stage pyrolysis of willow SRC at 520 °C using two heating rates: 25 °C/min (A) and 1500 °C/min (B). *Peak assignments*: (1) Acetic acid; (2) Toluene; (3) p-Xylene; (4) o-Xylene; (5) Phenol; (6) 2-Methylphenol; (7) 2-Methoxyphenol; (8) 1, 2-Benzenediol or/and Resorcinol; (9) 2,6-Dimethoxy-phenol; (10) 4-Ethylcatechol or/and 4-Ethyl-1,3-benzenediol; (11) 2,6-Dimethoxy-4-(2-propenyl)-phenol; (12) 2-Methoxy-4-methyl-phenol.

graph and MS-220 mass spectrometer. The column used was a Varian factorFOUR® (30 m, 0.25 mm id., 0.25 μm df). The gas chromatograph oven was held at 45 °C for 2.5 min and then ramped at 5 °C/min to 250 °C, with a dwell time of 7.5 min. The devolatised components were transferred via a heated transfer line maintained at 310 °C onto the GC column via an injector port held at 275 °C. Mass spectra were obtained for the molecular mass range $m/z = 45–300$. Proposed assignments of the main peaks were made from mass spectra detection using (NIST05 MS library) and from literature assignments [27,28].

2.2.3.2. Compound quantification. The GC column was calibrated using thirteen different compounds (purchased from Sigma Aldrich, UK). The compounds used for the calibration include: furan-2-carbaldehyde (furfural); 2-furanmethanol (furfuryl alcohol); phenol; 2-methoxyphenol (guaiacol); 2-methoxy-4-methylphenol (creosol); benzene-1,2-diol (catechol); 3-methoxycatechol (p-cresol), 1,2,4-trimethoxybenzene, 2-methoxy-4-vinylphenol; 4-allyl-2-methoxyphenol (eugenol), 4-hydroxy-3-methoxybenzaldehyde (vanillin), 1,6-anhydro-β-D-glucopyranose (levoglucosan) and 4-hydroxy-3,5-dimethoxybenzaldehyde (syringaldehyde). The stock solution was prepared using 0.5 ± 0.1 mg (Sartorius ME36S microbalance) of each compound, dissolved in GC-grade ethanol (Sigma–Aldrich, UK), in a 50 ml volumetric flask. The stock solution (10,000 μg/ml) was then diluted into five different concentrations (500, 800, 1200, 2000, and 4000 μg/ml) using GC-grade ethanol. 1 μl of each of the five calibration solutions was then separately analysed. The pyroprobe (set up for the final temperature of 280 °C at a heating rate of 100 °C/min) was used to evaporate each calibration solution. Evaporated compounds were transferred to the GC column via a heated transfer line (310 °C). The calibration curve was derived using the peak areas from each concentration versus the mass of the compound per 1 μl of solution. The calibration curve linearity (r^2) ranged between 0.9434 and 0.9983 for all compounds quantified. The same GC–MS parameters (oven temperature program and MS detector scan range) were applied for the compound quantification as for the analytical pyrolysis experiments.

2.2.4. Fast pyrolysis

The fast pyrolysis experiments were carried out in a bubbling 1 kg/h continuous bubbling fluidized bed reactor. The reactor setup and the liquid collection system are illustrated in Fig. 4a. The fluidizing gas was preheated nitrogen used on a single pass basis. The reactor bed material was 1 kg of quartz sand with a particle size between 710 and 850 μm. The experiments were carried out at an average reaction temperature of 500 °C. The residence time of the vapours in the hot reaction zone was below 1.5 s. The char particles were separated from the vapour and gas stream by two cyclones in series. The vapours were condensed in a cooled quench column using ISOPAR™ as quenching media at 30 °C. The aerosols were separated in a wet electrostatic precipitator flushed with ISOPAR™. Both condensates were collected in a common tank and are referred to as bio-oil. The ISOPAR™ was skimmed off at the top of this tank and recycled to the quench and electrostatic precipitator processes. The remaining condensable gases were condensed in a cascade of one water condenser at 10 °C and two dry ice condensers at −70 °C. The non-condensable gases were metered and analysed by a Varian CP 4900 Micro-GC for hydrocarbons up to C4. Temperatures were measured and recorded using a Microlink 751 ADC Unit combined with Windmill data logging software. The mass balance of the product yields was determined gravimetrically. The elaborate mass balancing procedure and the careful recovery of all output materials enable a mass balance closure of up to 95%. The water content of the liquids and the secondary condensates was determined by Karl Fisher volumetric titration in order to calculate reaction water.

2.2.5. Slow pyrolysis

Slow pyrolysis experiments were carried out in a batch reactor shown in Fig. 4b at 500 °C. The vapours were purged from the batch reactor with nitrogen at a flow rate of 100 cm^3/min and con-

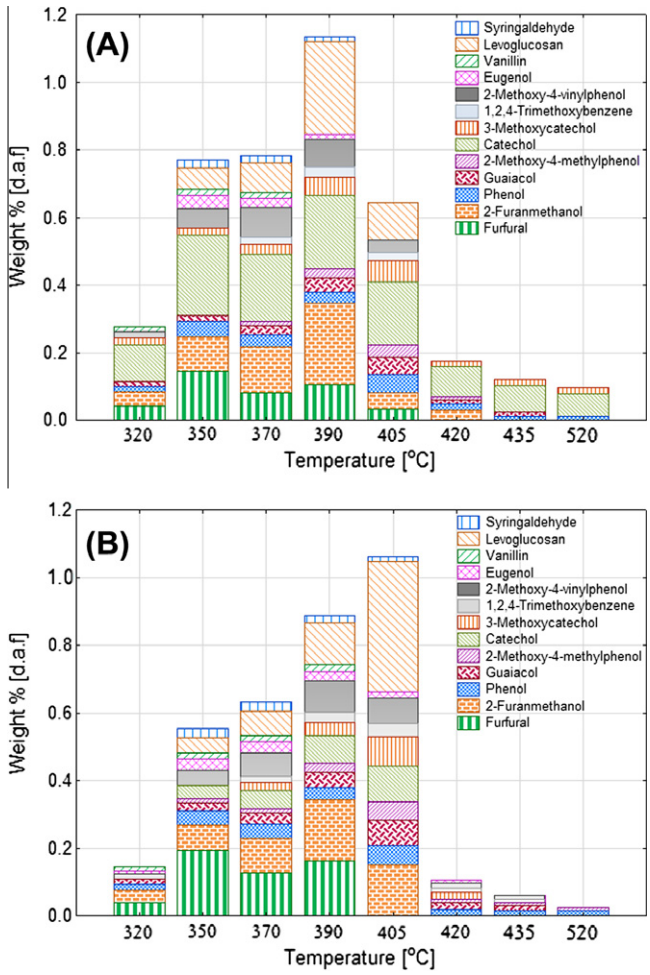

Fig. 9. Comparison of compound peak areas between 320 and 520 °C at two heating rates: 25 °C/min (A) and 1500 °C/min (B).

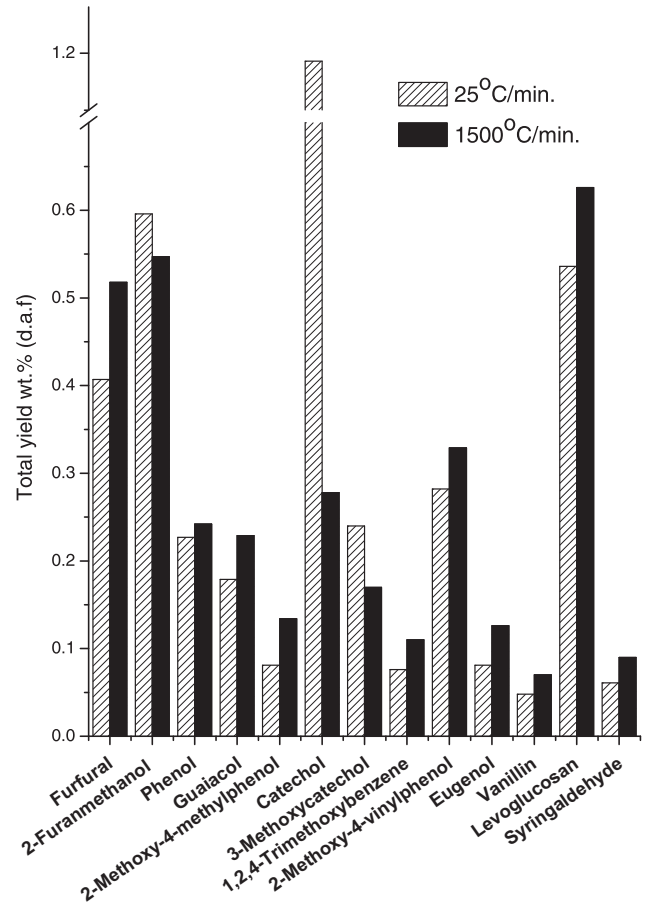

Fig. 10. Total yield of quantified compounds wt.%^{daf} at two heating rates (25 °C/min and 1500 °C/min) for each sequential pyrolysis experiment (320–520 °C).

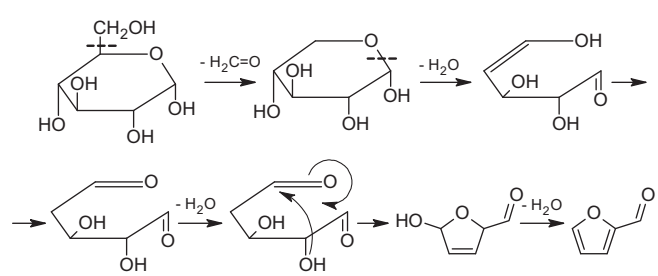

Fig. 11. Proposed pathway of the formation of furfural.

densed at 10 °C by a water condenser followed by two dry ice condensers at −70 °C. The non-condensable gases (NCG) were metered and analysed by a Varian CP 4900 Micro-GC for hydrocarbons up to C4. Temperatures were measured and recorded using a Microlink 751 ADC Unit combined with Windmill data logging software. The mass balance of the product yields was determined gravimetrically. The water content was determined by Karl Fisher titration in order to calculate reaction water.

2.2.6. GC–MS analysis of bio-oil

A PerkinElmer TurboMass Gold GC–MS/FID system was used for the analysis of the fast and slow pyrolysis bio-oil samples. GC samples were prepared by mixing bio-oil with GC grade 2-propanol (1:5 v/v). 1 µl of GC sample was injected onto the GC column via an injection port kept at 280 °C, with 1:25 split ratio. Separation was carried out on a PerkinElmer Elite-1701 column (Crossbond 14% cyanopropylphenyl – 86% dimethyl polysiloxane; 60 m, 0.25 mm i.d., 0.25 µm df). GC oven programme was as follows: held constant at 45 °C for 5 min, then ramped at 5 °C/min to 250 °C and held at 250 °C for 5 min Helium was used as carrier gas with a constant flow of 2 ml/min. Column splitter was used to enable simultaneous detection of separated on column compounds by MS and FID detectors. Mass spectra were obtained using 70 eV ionisation energy in the molecular mass range of m/z = 35–300. Proposed assignments of the main peaks were made from mass spectra detection using (NIST98 MS library) and from literature assignments [27,28]. The FID make-up gas was a mixture of hydrogen (45 ml/min) and air (450 ml/min). Detector temperature was 250 °C. Peak area under the FID chromatograms were used for quantification of bio-oil compounds.

3. Results and discussion

3.1. Biomass characterisation

Ultimate, proximate and inorganics analyses were carried out for willow SRC and are shown in Table 1. Proximate and ultimate results are typical for biomass material, oxygen content is very high and this is consistent with willow biomass polymeric constituents. Higher heating value was calculated using the equation proposed by Channiwala and Parikh (see Table 1) [26]. Oxygen content is known to be correlated to the calorific value, and this is apparent

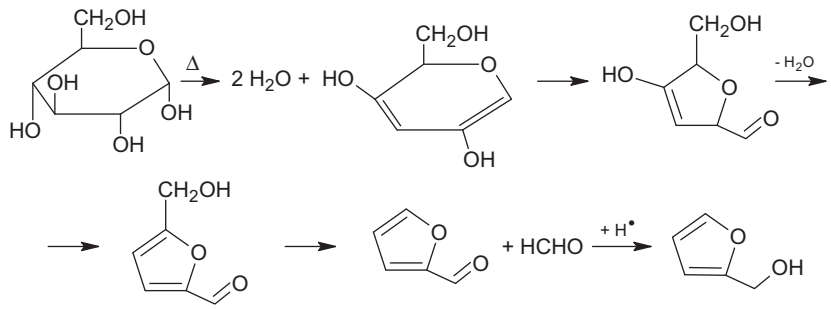

Fig. 12. Proposed pathway of the formation of 2-furanmethanol during the pyrolytic decomposition of levoglucosan at low heating rate.

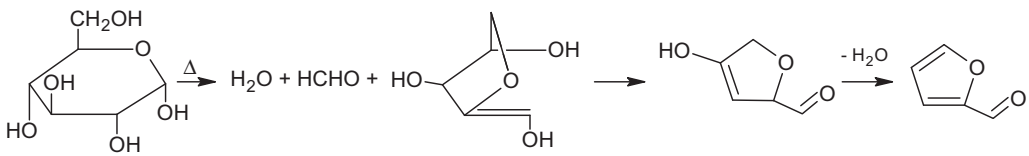

Fig. 13. Proposed pathway of the formation of furfural during the pyrolytic decomposition of levoglucosan at higher heating rate.

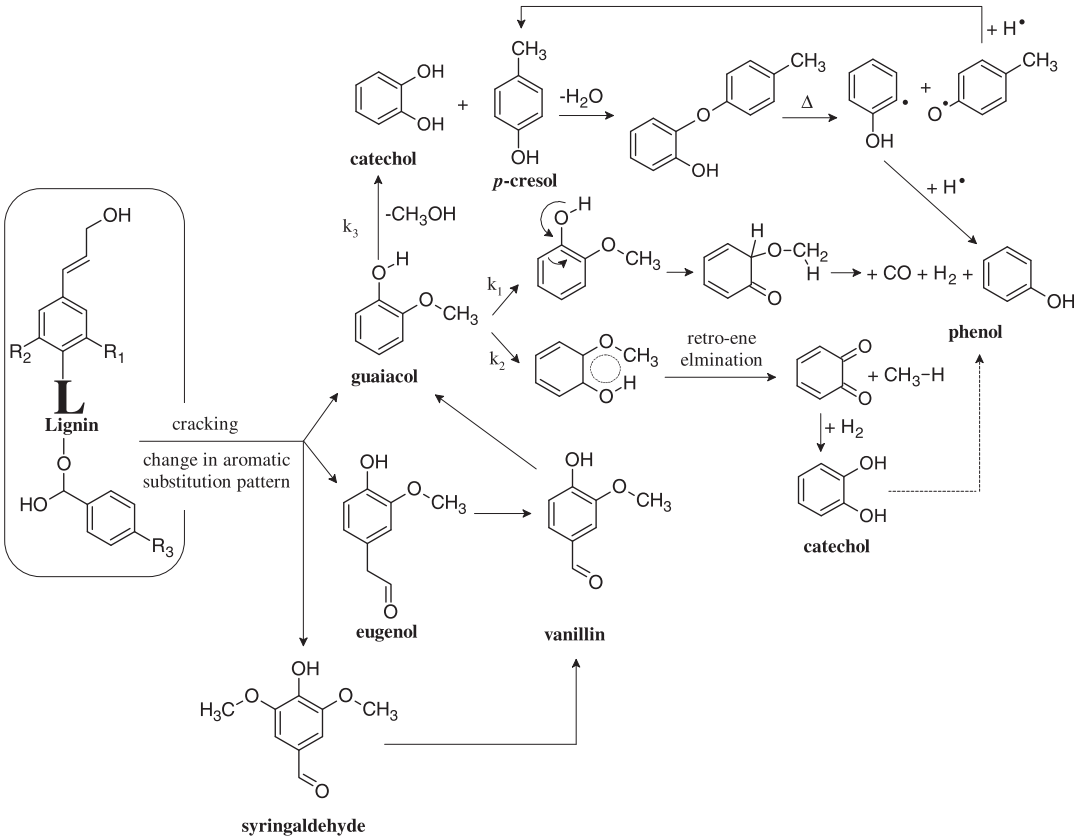

Fig. 14. Products from the pyrolytic decomposition of lignin.

because high oxygen content was detected and a low calorific value has been obtained. Thermogravimetric analysis in a nitrogen atmosphere was carried out and this is shown in Fig. 5. The maximum rate of weight loss occurs at 388 °C, at a rate of 13% per minute. A partial shoulder-like feature can be seen prior to the maximum rate of weight loss, and this is thought to be indicative of the hemicellulose content [29]. Ash content is representative of inorganic content and it has been found that calcium is the most abundant inorganic within willow SRC. The main inorganics found are shown in Table 1; these include calcium, potassium, phosphorous and magnesium.

3.2. Sequential pyrolysis (Py–GC–MS)

Analytical sequential pyrolysis (Py–GC–MS) was used to investigate product distribution, as a function of heating rate and pyrolysis temperature, in a stepped sequence, using single willow samples for each heating rate. Fig. 5 shows the TGA profile and

the main pyrolysis temperatures of interest (A–H). Table 2 presents thirteen chemical compounds and their weight percentage (on dry ash free basis), at eight different pyrolysis temperatures, using two different heating rates (25 and 1500 °C/min); representative of slow and fast pyrolysis. Of the sixteen chromatograms obtained, only six have been selected to show the most interesting differences. These can be found in the Figs. 6–8, at pyrolysis temperatures of 370, 405 and 520 °C (shown in Fig. 5 as C, E and H respectively). Two heating rates are shown in each figure to emphasise the difference in product distribution. Comparison of Figs. 6–8 reveals some interesting findings. Firstly, the chromatograms are different at their corresponding temperatures, and therefore product distribution is a function of temperature. This makes it possible, in principle, to carry out selective pyrolysis to acquire desired products, which is reported by Wu et al. [6]. Secondly, the chromatograms are different due to the use of different heating rates, and this adds to the ability to carry out selective pyrolysis as mentioned above.

A direct comparison of the two heating rates at different pyrolysis temperatures can be seen in Fig. 9, this is a graphical representation of the data in Table 2. Previous literature compliments the pattern of devolatisation found at different pyrolysis temperatures [5,6]. Fig. 10 shows the overall yield (d.a.f) between the two heating rates investigated, for each sequential pyrolysis experiment. For higher heating rates, yield increases were seen in the content of levoglucosan and furfural. Furfural, a furan derivative that is relatively similar in structure to 2-furanmethanol, is a pyrolytic decomposition product of levoglucosan. This was observed by Paine et al. [30], and is shown in Fig. 11. An inverse relationship between the yield of furfural and 2-furanmethanol can be seen when comparing the two heating rates (Fig. 10).

Kilzer and Broido [31] were able to propose a mechanism to support their claim, which was consistent with the energy release observed in char formation. They reported this to be a result of cross linking reactions by etherification and subsequent rearrangement, to produce water and a 5-hydroxymethylfurfural moiety. They also cited data to indicate that cross linking reactions for char formation are optimal at around 220 °C, and that higher temperatures around 400 °C resulted in significantly lower levels of char residue. Later work conducted by Weinstein and Broido [32] found that the crystalline region of cellulose and the mechanism of char formation are favourable to the plausibility of this mechanism. Lower heating rates promote further char formation. The elevated levels of hydroxymethylfurfural may contribute to the content of furfural and 2-furanmethanol. Char formation is believed to be associated with increased levels of free radicals. Shafizadeh and Lai [33], reported that low temperature pyrolysis of cellulose results in a decline in the degree of polymerisation, an increase in the level of free radicals, elimination of water, and the formation and evolution of carbonyl, carboxyl, hydroperoxide and aldehyde groups. Proton addition can result in the formation of 2-furanmenthanol from furfural, and this may be more favourable at lower heating rates. A possible formation pathway, at low heating rates, for furfural and 2-furanmethanol can be seen in Fig. 12. The proposed pathway produces an intermediate product known as hydroxymethylfurfural. The short residence times and reduced proton addition, seen at high heating rates, may favour an alternative decomposition pathway, that leads to the formation of furfural. A proposed pathway for the formation of furfural, at high heating rates, is shown in Fig. 13. This pathway does not produce a hydroxymethylfurfural intermediate. Subsequent proton addition, to the final furfural product in Fig. 13, could result in the formation of 2-furanmethanol.

In contrast to cellulose and hemicellulose, lignin decomposition occurs at higher temperatures and produces a range of phenolic compounds. The difference in overall yield wt.% (d.a.f), between low and high heating rates, can be seen in Fig. 10. For high heating rates, yield increases were seen for 2-methoxy-4-methylphenol, eugenol, vanillin, 1,2,4-trimethoxybenzene, syringaldehyde and guaiacol. The catechol content was found to be significantly higher at lower heating rates, and this was approximately three times higher than that obtained at higher heating rates. A derivative of catechol, 3-methoxycatechol also known as p-cresol, was also found to have a higher content at lower heating rates.

Fig. 14 shows the primary and secondary pyrolytic decomposition products from lignin. Guaiacol is thought to be a key intermediate for the production of catechol, p-cresol and phenol. Guaiacol can be formed either directly from lignin, or from other primary lignin decomposition products, e.g. eugenol and syringaldehyde. The numbers of secondary reactions are higher for lower heating rates because of the longer residence times. Longer residence times increase the number of decarboxylation, disproportionation and decarbonylation reactions. Therefore, at lower heating rates the content of primary decomposition products, such as guaiacol, eugenol and syringaldehyde, are expected to be low. This is evident when comparing the overall yield wt.% (d.a.f) for these compounds in Fig. 10. When comparing heating rate, minor differences were found in the content of phenol. It is possible that at higher heating rates the decomposition pathway to produce phenol could proceed through the pathway labelled k_1 on Fig. 14.

3.3. Laboratory scale pyrolysis

Fast and slow pyrolysis laboratory scale process conditions are shown in Table 3. The product yields and gas composition are given

Table 3
Fast and slow pyrolysis of willow SRC.

Operating conditions	Fast pyrolysis	Slow pyrolysis	Units
Average feeding rate	418.50	[a]	g/h
Biomass particle size	0.25–1.00	0.25–1.00	mm
Average pyrolysis temperature	500	500	°C
Run time	120	120	min
Biomass moisture content	6.50	13.58	%
Biomass used (d.b)	837.01	57.68	g
Hot vapour residence time	<1.5	>107	s
Quench liquid temperature	30	n/a	°C
Water condenser temperature	10	10	°C
Dry ice condenser temperature	−70	−70	°C

d.b – dry basis.
[a] Batch reactor fixed amount.

Table 4
Mass balance for fast and slow pyrolysis of willow SRC on dry basis.

Mass balance	Fast pyrolysis		Slow pyrolysis	
	g	%	g	%
Biomass	837.01		57.68	
Char total	161.37	**19.28**	34.54	**59.89**
Bio-oil total	429.74	**51.34**	16.10	**27.91**
Organics	339.11	40.51	7.81	13.55
Reaction water	90.63	10.83	8.28	14.36
Gas total	168.67	**19.89**	5.92	**10.26**
H_2	0.40	0.78	0.02	0.50
CO	65.65	9.22	1.57	3.26
CH_4	5.88	1.45	0.31	1.11
CO_2	86.22	7.71	3.63	4.79
Ethene	2.231	0.32	0.06	0.13
Ethane	0.33	0.16	0.09	0.18
Propene	3.35	0.19	0.08	0.11
Propane	1.82	0.04	0.08	0.11
n-Butane	2.78	0.02	0.07	0.07
Closure	-	**90.51**	-	**98.06**

Table 5
Comparison of laboratory scale fast and slow pyrolysis bio-oil composition.

Retention time (min)	Compound name	Fast pyrolysis	Slow pyrolysis
		Peak area (%)	Peak area (%)
6.67	Acetic acid, anhydride with formic acid	–	5.00
10.80	Acetic acid	20.42	5.10
11.60	Acetic acid, methyl ester	14.70	15.90
12.12	3-Hydroxy-2-butanone	0.18	–
12.2	3-Hydroxy-2-butane	–	8.03
13.46	Furfural	2.06	7.23
14.48	1,4-Dimethyl-pyrazole	2.50	–
14.75	1,3-Cyclohexanediol	1.90	–
15.05	2-Methyl-furan	1.56	–
15.58	Hexanoic acid	0.61	–
16.22	1-(Acetyloxy)-2-propanone	1.16	–
16.60	2-Furnamethanol	–	2.95
16.61	2-Methyl-2-cyclopenten-1-one	0.26	–
16.95	2-Methyl-propanoic acid	0.43	–
17.42	2-Ethyl-3-methyl-2-pentanol	0.05	–
17.73	2-Butenoic acid	0.17	–
18.99	2-Hydroxy-2-cyclopenten-1-one	–	4.00
19.20	4-Hydroxy-butanoic acid	1.13	–
19.40	2- and/or 3-Methyl-2-cyclopenten-1-one	0.70	–
19.48	Dihydro-4-methyl-2(3H)-furanoneand/or 2,4-dimethyl-cyclopentanone	-	1.13
19.74	Cyclopentanone	1.95	–
19.91	3,4-Dimethyl-2-pentene	0.43	–
20.86	4-Methyl-2-pentene	0.64	–
21.60	Phenol	7.10	0.46
21.86	2-Hydroxy-3-methyl-2-cyclopenten-1-one	–	3.89
22.48	2-Methoxy-phenol or/and menquinol	1.54	0.63
22.99	2-Methyl-phenol	0.27	–
23.16	2-(2-Propenyl)-furan	0.33	–
23.91	3-Ethyl-2-hydroxy-2-cyclopenten-1-oneand/or 3,4-dimethyl-2-hydroxy-cyclopenten-2-en-1-one	–	1.21
24.39	Maltol	0.29	0.66
27.50	4-Ethly-2-methoxy-phenol	0.30	–
28.33	2,3- and/or 3,4-Anhydrogalactosan	0.70	0.57
28.73	1,4:3,6-Dianhydro-α-D-glucopyranose	–	0.42
28.86	1-(2-Hydroxy-methylphenyl)-ethanone	0.35	–
28.91	2-Methoxy-4-vinylphenol	–	0.28
29.54	Eugenol	0.38	–
30.46	2,6-Dimethoxyphenol	4.91	4.31
32.16	2-Methoxy-4-(1-propenyl)-phenol	0.28	0.54
32.54	1,2,4-Trimethoxybenzene	1.73	1.83
32.76	Vanillin	1.45	0.27
34.17	1,2,3-Trimethoxy-5-methyl-benzene	0.41	0.98
34.64	1-(4-Hydroxy-3-methoxyphenyl)-ethanone	0.87	0.23
35.58	2-Methoxy-4-propenyl-phenol	0.23	–
35.89	2,6-Dimethoxy-4-(2-propenyl)-phenol	0.37	0.52
35.91	2,5-Dimethoxy-ethylbenzene	1.09	0.25
36.98	2,5-dimethoxy-4-ethylbenzaldehyde	–	0.25
38.26	2,4,6-Trimethoxystyrene	–	1.15
38.92	4-Hydroxy-3,5-dimethoxy-benzaldehyde	1.20	0.70
40.33	1-(4-Hydroxy-3,5-dimethoxyphenyl)-ethanone	1.15	0.46
41.06	1-(2,4,6-Trihydroxyphenyl)-2-pentanone	0.70	1.43
	Total (%)	76.50	70.38

– Not detected.

in Table 4. A mass balance closure of 91% was achieved for fast pyrolysis and 98% for slow pyrolysis. The main bio-oil generated was compared using GC–MS/FID and the results can be found in Table 5. The chemical analysis of the liquids show a high level of accountability, with over 70% of the peak area in both cases having chemical assignments. The analyses show high yields of acetic acid and methyl acetate from fast pyrolysis, as well as significant yields of phenol and 2,6-dimethoxyphenol. Notable in the slow pyrolysis organic fraction are high yields of methyl acetate, 3-hydroxy-2-butane, furfural and cyclopenentes, which is a final decomposition product of cellulose pyrolysis.

Acceptable mass balance closures were obtained in both cases. The lower figure for fast pyrolysis is typical of closures on this unit, due to liquid hold up and high nitrogen content in the gas leading to gas analysis errors. The very high char yield in slow pyrolysis is due to the relatively low temperature in non-oxidising carbonisation, and the relatively short reaction time for a finely ground biomass sample, with the possibility for adsorption and cracking of liquid precursors on the produced char.

4. Conclusions

Analytical and laboratory scale pyrolysis have been used to produce pyrolysis products from willow. Analytical sequential pyrolysis using two different heating rates has been shown to influence product quantity and distribution. A combination of a specific pyrolysis temperature and heating rate will increase the possibilities for targeting more desirable chemicals. A number of interesting correlations were found between compounds at different heating rates over a range of different pyrolysis temperatures. The chemical composition of the bio-oil produced (fast and slow

pyrolysis) shows notable differences. Optimisation of the pyrolysis process is an essential step to develop this technology.

Acknowledgements

The authors are grateful for the financial support from the SUPERGEN Bioenergy Consortium under the EPRSC Research Grant "SUPERGEN Biomass Biofuels and Energy Crops II Core" No. EP/E039995/1. The authors are grateful for the supply of willow SRC by Rothamsted Research, Harpenden, UK, a partner in SUPERGEN Bioenergy Consortium. The authors would also like to thank Dr. G. Jiang for his contribution to the GC-MS/FID quantification work carried out.

References

[1] Boyd J, Dinkelbach L, Chriserson L. The scottish agricultural college alterner report 'Energy from willow'. Edinburgh, UK; 2000.
[2] Bridgwater A. Review of fast pyrolysis of biomass and product upgrading. Biomass Bioenergy 2011:1–27.
[3] Bridgwater AV, Peacocke C. Fast pyrolysis processes for biomass. Renew Sust Energ Rev 2000;4:1–73.
[4] Gerdes C. Pyrolyse von biomasseabfall. Thermochemische konversion mit dem hamburger wirbelschichtverfahren. Hamburg: Universität Hamburg; 2001. [cited 18.01.11]. <http://deposit.ddb.de/cgi-bin/dokserv?idn=964083507>.
[5] Alén R, Kuoppala E, Oesch P. Formation of the main degradation compound groups from wood and its components during pyrolysis. J Anal Appl Pyrolysis 1996;36:137–48.
[6] Wu Y, Zhao Z, Li H, He F. Low temperature pyrolysis characteristics of major components of biomass. J Fuel Chem Technol 2009;37:427–32.
[7] Radlein D, Piskorz J, Scott DS. Fast pyrolysis of natural polysaccharides as a potential industrial process. J Anal Appl Pyrolysis 1991;19:41–63.
[8] Piskorz J, Radlein D, Scott DS, Czernik S. Liquid products from the fast pyrolysis of wood and cellulose. In: Bridgwater AV, Kuester JL, editors. Research in thermochemical biomass conversion. Elsevier Applied Science; 1998. p. 557–71.
[9] Bradbury AGW, Sakai Y, Shafizadeh F. A kinetic model for pyrolysis of cellulose. J Appl Polym Sci 1979;23:3271–80.
[10] Liao Y, Wang S, Ma X. Study of reaction mechanism in cellulose pyrolysis. Prep Pap Am Chem Soc Div Fuel Chem 2004;49:409–11.
[11] Antal MJ, Varhegyi G. Cellulose pyrolysis kinetics: the current state of knowledge. Ind Eng Chem Res 1995;34:703–17.
[12] Antal MJ, Mok WSL, Roy JC, Raissi AT, Anderson DGM. Pyrolytic source of hydrocarbons from biomass. J Anal Appl Pyrolysis 1985;8:291–303.
[13] Antal MJ. A review of the literature, part i, carbohydrate pyrolysis. Adv Sol Energy 1982;1:61–111.
[14] Ponder GR, Richards GN. A review of some recent studies on mechanisms of pyrolysis of polysaccharides. Biomass Bioenergy 1994;7:1–24.
[15] Roberts VM, Stein V, Reiner T, Lemonidou A, Li X, Lercher JA. Towards quantitative catalytic lignin depolymerisation. Chem – A Eur J 2011;17:5939–48.
[16] Westerhof RJM, Brilman DWF, Swaaij WPM, Kersten SRA. Effect of temperature in fluidized bed fast pyrolysis of biomass: oil quality assessment in test units. Ind Eng Chem Res 2009;49:1160–8.
[17] Nowakowski DJ, Woodbridge CR, Jones JM. Phosphorus catalysis in the pyrolysis behaviour of biomass. J Anal Appl Pyrolysis 2008;83:197–204.
[18] Mani T, Murugan P, Abedi J, Mahinpey N. Pyrolysis of wheat straw in a thermogravimetric analyzer: effect of particle size and heating rate on devolatilization and estimation of global kinetics. Chem Eng Res Des 2010;88:952–8.
[19] Coats AW, Redfern JP. Kinetic parameters from thermogravimetric data. Nature 1964;201:68–9.
[20] Lapuerta M, Hernández JJ, Rodríguez J. Kinetics of devolatilisation of forestry wastes from thermogravimetric analysis. Biomass Bioenergy 2004;27:385–91.
[21] Deng N, Zhang Y, Wang Y. Thermogravimetric analysis and kinetic study on pyrolysis of representative medical waste composition. Waste Manage 2008;28:1572–80.
[22] Kumar A, Wang L, Dzenis YA, Jones DD, Hanna MA. Thermogravimetric characterization of corn stover as gasification and pyrolysis feedstock. Biomass Bioenergy 2008;32:460–7.
[23] Park Y-H, Kim J, Kim S-S, Park Y-K. Pyrolysis characteristics and kinetics of oak trees using thermogravimetric analyzer and micro-tubing reactor. Bioresour Technol 2009;100:400–5.
[24] Gronli M, Antal Jr M, Varhegyi G. A round-robin study of cellulose pyrolysis kinetics by thermogravimetry. Ind Eng Chem Res 1999;38:2238–44.
[25] ASTM Standard E 1131-03 – Test method for compositional analysis by thermogravimetry. ASTM International; 2003.
[26] Channiwala S, Parikh P. A unified correlation for estimating HHV of solid, liquid and gaseous fuels. Fuel 2002;81:1051–63.
[27] Faix O, Fortmann I, Meier D. Gas chromatographic separation and mass spectrometric characterization of monomeric lignin derived products. Holz als Rohund Werkstoff 1990;48:281–5.
[28] Faix O, Fortmann I, Bremer J, Meier D. Gas chromatographic separation and mass spectrometric characterization of polysaccharide derived products. Holz als Roh-und Werkstoff 1991;49:213–9.
[29] Vamvuka D, Kakaras E, Kastanaki E, Grammelis P. Pyrolysis characteristics and kinetics of biomass residuals mixtures with lignite. Fuel 2003;82:1949–60.
[30] Paine J, Pithawalla YB, Naworal JD. Carbohydrate pyrolysis mechanism from isotopic labelling: part 4. The pyrolysis of D-glucose: the formation of furans. J Anal Appl Pyrolysis 2008;83:37–63.
[31] Broido A, Kilzer FJ. A critique of the present state of knowledge of the mechanism of cellulose pyrolysis. Fire Res 1963;5:157.
[32] Weinstein M, Broido A. Pyrolysis-crystallinity relationships in cellulose. Combust Sci Technol 1970;1:287.
[33] Shafizadeh F, Lai YZ. Thermal degradation of 1,6-anhydro-. beta.-D-glucopyranose. J Org Chem 1972;37:278–84.